경수로용 핵연료집합체 지지격자의 좌굴특성에 관한 연구

A Study on the Buckling Characteristics of Spacer Grids in Pressurized Water Reactor Fuel Assembly

전 상 윤† 이 영 신*
Jeon, Sang-Youn Lee, Young-Shin

(논문접수일 : 2004년 12월 30일 : 심사종료일 : 2005년 9월 29일)

요 지

본 연구에서는 경수로용 핵연료집합체의 전체지지격자(Full Size Grid)와 부분지지격자(Small Size Grid)에 대한 정적 좌굴강도 실험과 전체 지지격자와 부분지지격자를 구성하는 지지격자판(Grid Strap)에 대한 정적 좌굴해석을 수행하여 지지격자의 좌굴특성을 분석하였으며, 분석결과를 이용하여 전체지지격자와 부분지지격자에 대한 좌굴하중값의 예측 가능성을 평가하였다. 좌굴강도 실험은 웨스팅하우스형 연료의 17×17셀을 갖는 전체지지격자와 1×1, 1×2, 1×3, 1×4, 1×5, 1×17, 2×1, 2×2, 2×3, 2×9, 2×17, 3×17 등의 셀을 갖는 부분지지격자에 대하여 수행하였으며, 실험결과를 이용하여 지지격자의 좌굴강도와 지지격자의 행(rows)과 열(columns) 사이의 관계식을 제시하였다. 좌굴강도 해석은 범용 유한요소해석코드인 ANSYS를 이용하여 수행하였으며, 해석결과를 이용하여 지지격자의 좌굴특성을 분석하고 실험결과와 비교평가하였다.

핵심용어 : 가압경수로, 핵연료집합체, 지지격자, 판, 좌굴강도, 좌굴모드

Abstract

This study contains the static buckling tests and static buckling analyses for small size grids and full size grids. The buckling tests and finite element analyses were performed to evaluate the buckling characteristics of the spacer grids in a pressurized water reactor fuel assembly and to evaluate the possibility of the prediction for the buckling strength of spacer grids. The buckling tests were performed for small size grids and full size grids, and the correlations between buckling strength and the number of straps and the correlations between buckling strength and the number of rows are derived based on the test results. The static buckling analyses were performed to identify the effect of the number of rows and the number of columns on the buckling strength of spacer grid by a finite element method using ANSYS program and the results were compared with the buckling test results.

keywords : *pressurized water reactor, fuel assembly, spacer grid, full size grids, small size grids, buckling strength, buckling mode*

1. Introduction

The spacer grids of pressurized water reactor fuel assembly support the fuel rods along their length and maintain the lateral spacing between the rods throughout the design life of the fuel assembly. The fuel rod of the 17×17 type fuel assembly considered in this study is supported at six points within each grid cell by a combination of springs and dimples. Each grid is composed of interconnected array of slotted grid straps, that are welded at the intersections to form a lattice like plate structure(KNFC, 1994) as shown in Fig. 1. The spacer grid impacts with the baffle plate and/or spacer grid of neighboring fuel assemblies during the seismic and LOCA(Loss of Coolant Accident). The spacer grid should maintain the lateral spacing between the rods under both the

† 책임저자, 정회원 · 한전원자력연료㈜ 설계기술원 책임연구원
전화: 042-868-1182 : Fax: 042-868-1149
E-mail: syjeon@knfc.co.kr
* 정회원, 충남대학교 기계설계공학과 교수

• 이 논문에 대한 토론을 2006년 3월 31일까지 본 학회에 보내주시면 2006년 6월호에 그 결과를 게재하겠습니다.

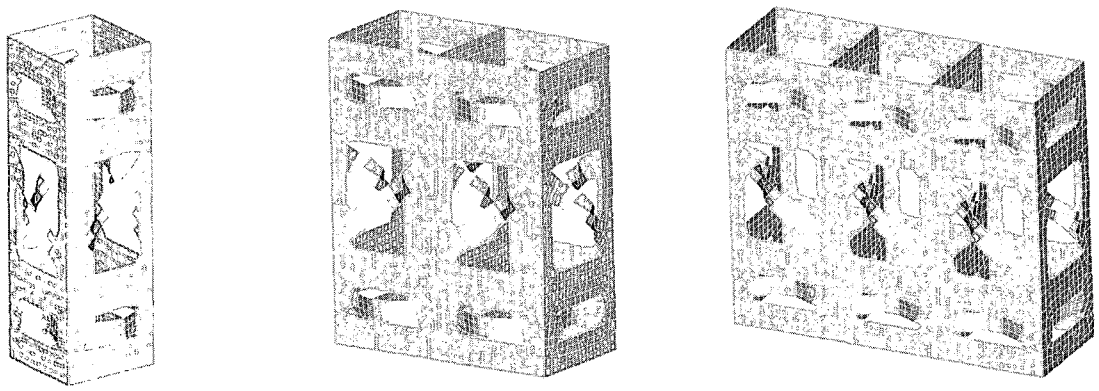

(1X1) (1X2) (1X3)

(a) Small Size Grids

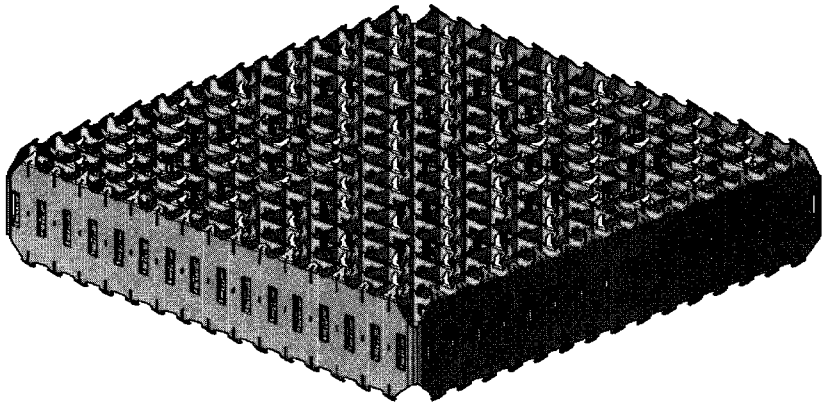

(b) Full Size Grid

Fig. 1 The Configuration of Small Size Grids and Full Size Grid

operational and the accident loading conditions, such as seismic and LOCA, to maintain the coolability of the reactor core geometry(USNRC, 1981). The impact test of spacer grid has been performed at an operating temperature to verify the requirements for accident conditions. Hyun(1997) performed a study on the fatigue and buckling/ultimate strength of new slot hole structure(Hyun 등, 1997). Heo(1999) investigated the effects of lamination mechanism, fiber orientation angle and stacking sequence, etc. on the buckling and post-buckling behaviors of laminated composite plates and stiffened laminated composite panels(Heo 등, 1999) Yoon(2001) investigated the nonlinear dynamic buckling behavior of a partial spacer grid assembly considering that the spacer grid is an assembled structure with thin-walled plates(Yoon 등, 2001). Lee(2002) proposed a theoretical model based on a generalized variational principle for magneto-thermo-elasticity to describe the coupled magneto-thermo-elastic interaction in soft ferromagnetic plates. The effects of thermal and magnetic fields on the magneto-thermo-elastic bending and buckling are investigated(Lee 등, 2002). Lee (2002) performed the stability analysis of the plate under different loading conditions by the finite element method. The parameters considered in the analysis are aspect ratio and patch load width factor(Lee 등, 2002). Han(2004) performed parametric study with finite element method and proposed a simplified formula and shear buckling coefficients for the design of curved web panels(Han 등, 2002). Park(2004) developed the formulas using finite element method for the buckling and compressive ultimate strength of rectangular plate with cutout (Park 등, 2004).

In development of new spacer grids design, several different grid designs might be proposed

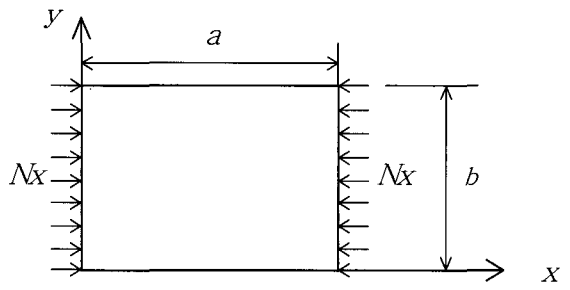

Fig. 2 Simply Supported Rectangular Plate

during the very early stage of the development. The performance of each grid design will be evaluated by analysis and test to choose the best design. One of the important performances of the spacer grid is buckling characteristic of the grid for the structural evaluation of the seismic and LOCA load. To evaluate the buckling characteristics, the proposed design need to be tested with the small size grid instead of the full size grid due to the higher manufacturing cost and longer manufacturing period for the full size grid. The understanding of the correlation between the buckling strength and the design variables of grid will be helpful for the evaluation of the buckling strength of the final product.

In this study, the static buckling tests and finite element analyses for small size grids and full size grids were performed to evaluate the buckling characteristics of the spacer grids. The buckling tests were performed for the full size grids, 17×17, and the small size grids having several different number of spacer grid rows and columns, e.g. 1×1, 1×2, 1×3, 1×4, 1×5, 1×17, 2×1, 2×2, 2×3, 2×9, 2×17, 3×17. Based on the test results, the buckling characteristics of spacer grids were evaluated, and the correlations between buckling strength and the number of straps and the correlations between buckling strength and the number of rows were derived. The static buckling analyses were performed to identify the effect of the number of rows and the number of columns on the buckling strength of spacer grid by a finite element method using ANSYS program(ANSYS Rev. 5.6) and the results were compared with the experimental test results.

2. Buckling of Rectangular Plate

When a simply supported rectangular plate is subjected to uniaxial in-plane forces, N_x, as shown in Fig. 2, the minimum critical load can be written as follows(Timoshenko 등, 1982) :

$$(N_x)_{cr} = \frac{\pi^2 D}{b^2}\left(\frac{b}{a}+\frac{a}{b}\right)^2 \quad (1)$$

where, (Nx)cr : Critical Compressive Load per Unit Distance,

$D = Et^3/12(1-\nu^2)$: Flexural Rigidity,
E : Elastic Modulus, ν : Poisson's Ratio,
a : Width of the Plate, b : Height of the Plate,
t : Thickness of the Plate

The above equation is applicable to the simply supported rectangular isotropic plate subjected to uniaxial in-plane forces. In case of spacer grid strap, the geometrical shape and boundary conditions are somewhat different from the rectangular plate that is considered in equation (1). Several windows and horizontal slots exist for spring and dimples on the each strap of spacer grid. There are also several vertical slots at upper part or lower part of the strap to assemble the straps for the fabrication of the grid assembly. And, the straps are welded at the intersections to fabricate the grid assembly. It can be said that the boundary conditions are the combination of simply supported and clamped conditions due to the slots for the assembling of the straps and welding at the top and bottom intersections of the straps. Therefore, the above equation cannot be directly used for the study of grid buckling analyses, but it is presumed that the buckling strength is proportional to third power of plate thickness and depends on the ratio of a/b. In this study, the buckling strengths of the grid strap were calculated using a commercial finite element program, ANSYS, and the results are compared with the buckling strengths from the static buckling

Table 1 Test Matrix of Small Size Grids and Full Size Grids

Items		Quantity (EA)
Small Size Grids	1 ROW (1×1, 1×2, 1×3, 1×4, 1×5, etc.)	26
	2 ROW (2×1, 2×2, 2×3, 2×9, etc.)	20
	3 ROW (3×17)	4
Full Size Grids	17 ROW (17×17)	5

Table 2 Mechanical Properties of Grid Strap

Items	Values
Material	Zircaloy-4
Young's Modulus (at 70°F, psi)	14.3×10^6
Poisson Ratio	0.3
Yield Strength, 0.2% (Minimum, psi)	43,000
Ultimate Tensile Strength (Minimum, psi)	55,000

Table 3 Static Buckling Test Results

Grid Type	Buckling Strength (lbf)	Grid Type	Buckling Strength (lbf)
1×1	659	2×1	304
1×2	982	2×2	448
1×3	1,315	2×3	654
1×4	1,634	2×9	1,697
1×5	1,931	2×17	3,509
1×17	5,762	3×17	2,663
		17×17	1,618

(Note) Buckling strengths are the average of 3 to 5 samples.

tests to evaluate the buckling characteristics of the spacer grid.

3. Static Buckling Tests and Results

Five full size grids and fifty small size grids were prepared for the static buckling test. Fig. 1 shows the configuration of the small size grids (1×1, 1×2, 1×3) and full size grid (17×17). The detailed geometrical dimensions of the straps consisting of small size grids and full size grid are shown in Fig. 9. The full size grids are sectioned into small size grids. All the small size grids consist of inner strap only except 17 column grids. The 17 column and full size grids contain the outer straps at the peripheral location of the grid. Table 1 shows the number of small size grids and full size grids used in static buckling test. The configuration of test setup is shown in Fig. 3. Fig. 4 shows the shape of small size grids and full size grids after buckling test. The mechanical properties for the spacer grid straps are given in Table 2(KNFC, 1994). The buckling tests for small size grids and full size grids were performed using universal test machine. The compressive loads acting on the grids were measured as a function

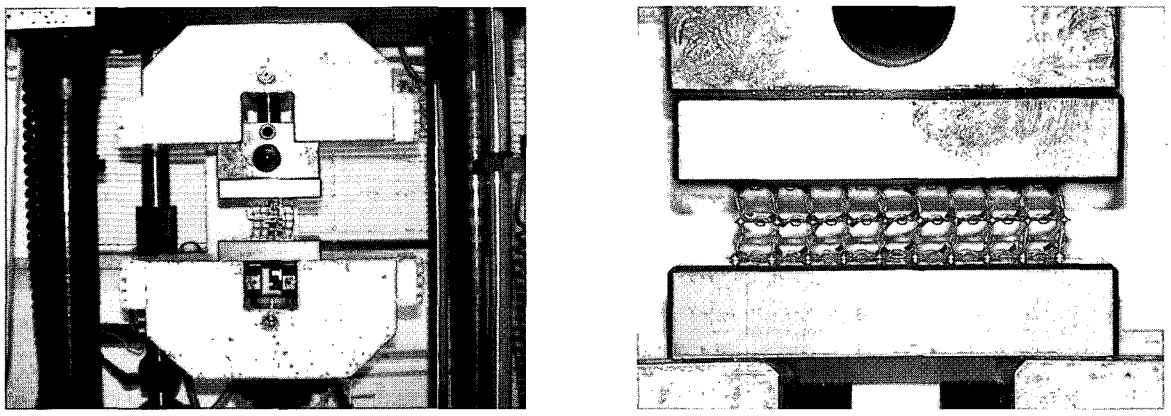

Fig. 3 Configuration of Test Setup

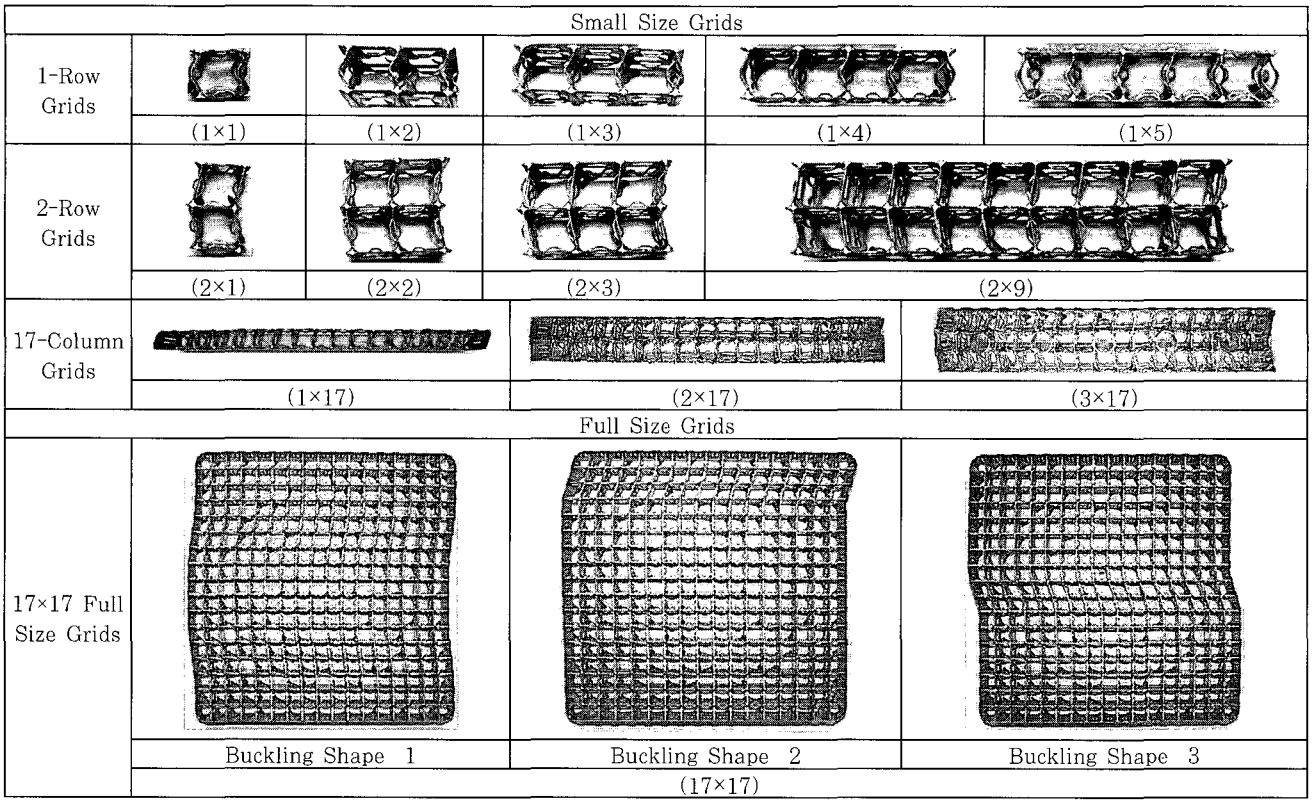

Fig. 4 The Buckling Shapes of Small Size Grids and Full Size Grids

of deflection during the buckling test. The buckling strengths are summarized in Table 3 and the buckling shapes are shown in Fig. 4.

The buckling strengths of small size grids as a function of the number of straps (number of columns+1) for the cases of 1 and 2 rows are shown in Fig. 5. The correlation between buckling strength and the number of straps for 1 row and 2 row cases can be written as the following equations based on the average buckling strength from test results.

$$Fs = 318.47\,Ns + 29.965 \quad \text{for 1 row case} \tag{2}$$

$$Fs = 199.61\,Ns + 154.94 \quad \text{for 2 row case} \tag{3}$$

where, Fs : Buckling Strength as a function of the number of Straps, lbf

Ns : Number of Straps (number of columns+1)

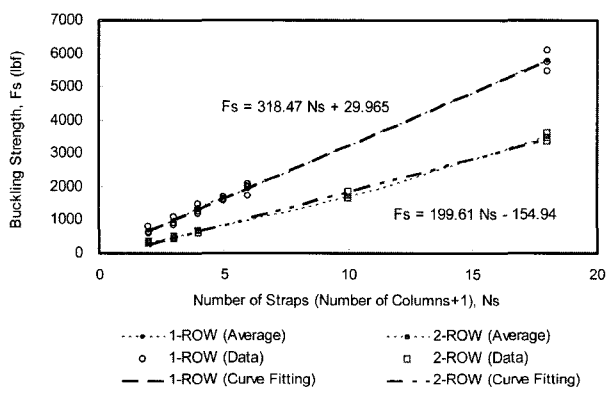

Fig. 5 Buckling Strengths as a function of the Number of Straps (Test Result)

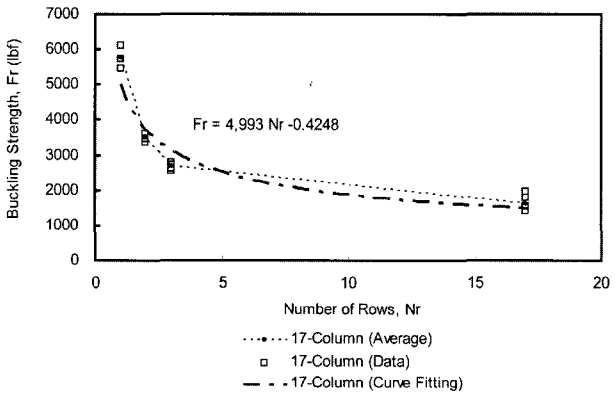

Fig. 6 Buckling Strengths as a function of the Number of Rows (Test Result)

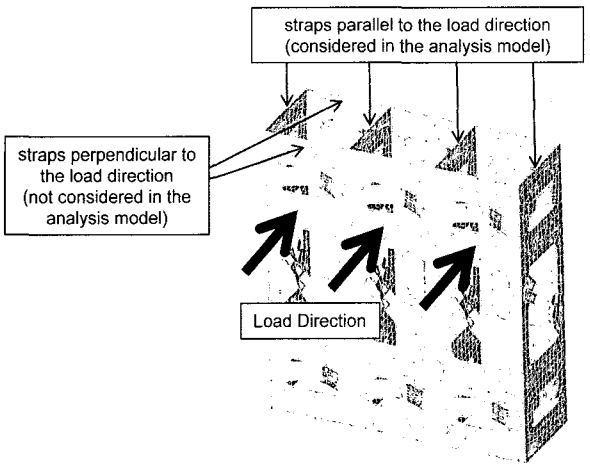

Fig. 7 Straps considered in the Finite Element Models

Fig. 6 shows the buckling strengths of grids as a function of the number of rows for the case of 17 columns. The correlation between buckling strength and the number of rows for 17 columns are shown as the following equation based on the average buckling strength from test results.

$$Fr = 4{,}993\ Nr^{-0.4248} \tag{4}$$

where, Fr : Buckling Strength as a function of the number of Rows, lbf

Nr : Number of Rows

4. Static Buckling Analysis and Results

The finite element analyses were performed to identify the effect of the number of rows and the number of columns on the buckling strength of full size grid and small size grids having several different number of spacer grid straps using simplified strap models. The eigenvalue buckling analyses were carried out using subspace method in ANSYS program. A 3-dimensional finite element models might be needed for the buckling analysis of the small size grid. In general, the buckling of the grid occurs in the straps parallel to the load direction, on the other hand there is no buckling or deformation in the straps perpendicular to the load direction. Based on the buckling shapes of test results, it was evaluated that the simplified strap model can be used for the buckling analysis.

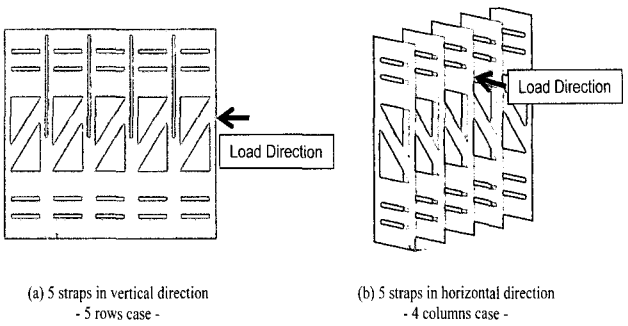

Fig. 8 Example of Simplified Strap Models

The straps which are parallel to the load direction, as shown in Fig. 7, are considered as a finite element model for the buckling analysis. The straps perpendicular to the load direction, as shown in Fig. 7, are not considered for the analysis model because the straps perpendicular to the load direction don't play any important roles for the buckling strength of grid. The effects of the straps perpendicular to the load direction are considered as boundary conditions, such as coupling and constraints. For the evaluation of the effects of the number of columns and rows, the simplified strap models were generated for 1, 2, 3, 4, and 5 straps in horizontal direction (perpendicular to the load direction) and 1, 2, 3, 4, and 5 straps in vertical direction (parallel to the load direction). The simplified strap models of 2, 3, 4, and 5 straps in horizontal direction are for the buckling analyses of 1, 2, 3, and 4 columns of small size grids, respectively. The simplified strap models of 1, 2, 3, 4, and 5 straps in vertical direction are for the buckling analyses of 1, 2, 3, 4, and 5 rows of small size grids, respectively. Fig. 8(a) and (b) shows the example of the simplified strap models in vertical and horizontal directions. Fig. 8(a) shows the 5 straps model in vertical direction (for 5 rows grids) and Fig. 8(b) shows the 5 straps model in horizontal direction (for 4 columns grids). Fig. 9 shows the geometrical dimensions of simplified strap models for the buckling analysis of the grids. The strap models for the finite element analyses are generated with inner strap thickness. The effects of the outer straps on the evaluation

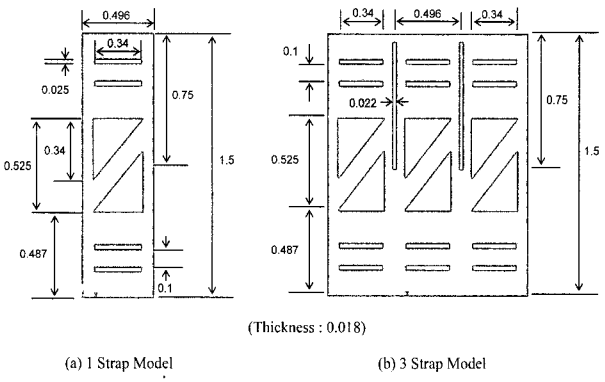

Fig. 9 Geometrical Dimensions of Simplified Strap Models (unit : inches)

of the buckling analysis results are not considered.

The finite element models consist of 4 node quadrilateral elastic shell elements, SHELL63. Each cell of the strap models consists of 1,545 elements and 1,773 nodes. Fig. 10 shows the shape of strap models and boundary conditions that are used for the static buckling analyses. The static buckling analyses were performed with the three different boundary conditions, clamped-clamped, clamped free, and hinged hinged boundary conditions, as described in Fig. 10. The clamped-clamped boundary condition was used to consider the buckling shapes of small size grids from the test results. Both ends of small size grids are not moved in lateral direction based on the buckling shapes of 1, 2, and 3 row grids in Fig. 4. The clamped-free boundary condition was used to consider the buckling shapes of full size grids. The buckling shapes of full size grid were strap buckling at 3 to 4 rows and there were lateral movements of straps as shown in Fig. 4. The hinged-hinged boundary condition was additionally used to evaluate the buckling shapes of 1 row grids. The combination of simply supported and clamped boundary conditions was used for the boundary condition of grid strap models to consider the supporting effects by the slot of strap perpendicular to the load direction. The simply supported conditions are applied for the upper part (Region B and E in Fig. 10) of the strap to

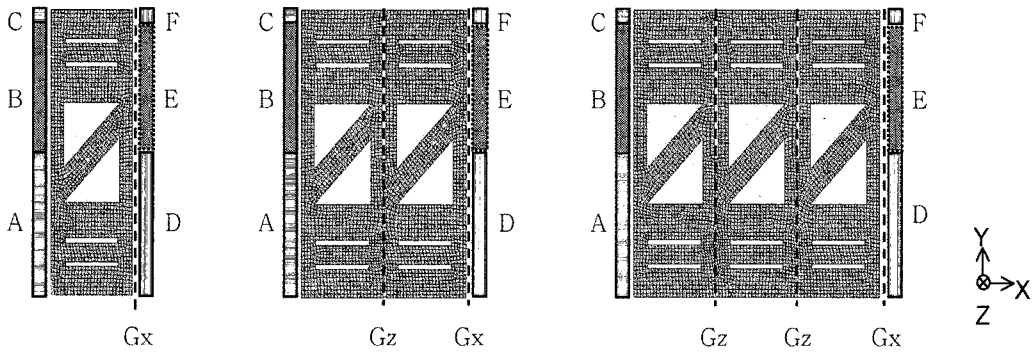

Region Gx : Displacement Coupling with Ux, Region Gz : Displacement Coupling with Uz

For Clamped Clamped Boundary Condition

Region A : Ux=Uy=Uz=Rx=Ry=Rz=0, Region B : Ux=Uy=Uz=0, Region C : Ux=Uy=Uz=Rx=Ry=Rz=0,
Region D : Uy=Uz=Rx=Ry=Rz=0, Region E : Uy=Uz=0, Region F : Uy=Uz=Rx=Ry=Rz=0

For Clamped Free Boundary Condition

Region A : Ux=Uy=Uz=Rx=Ry=Rz=0, Region B : Ux=Uy=Uz=0, Region C : Ux=Uy=Uz=Rx=Ry=Rz=0,
Region D : Uy=Rx=Ry=Rz=0, Region E : Uy=0, Region F : Uy=Rx=Ry=Rz=0

For Hinged Hinged Boundary Condition

Region A : Ux=Uy=Uz=Rx=Rz=0, Region B : Ux=Uy=Uz=0, Region C : Ux=Uy=Uz=Rx=Rz=0,
Region D : Uy=Uz=Rx=Rz=0, Region E : Uy=Uz=0, Region F : Uy=Uz=Rx=Rz=0

Fig. 10 Finite Element Models and Boundary Conditions

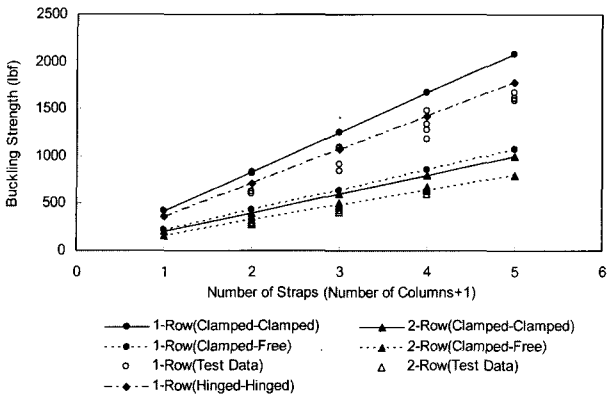

Fig. 11 Buckling Strengths as a function of the Number of Columns

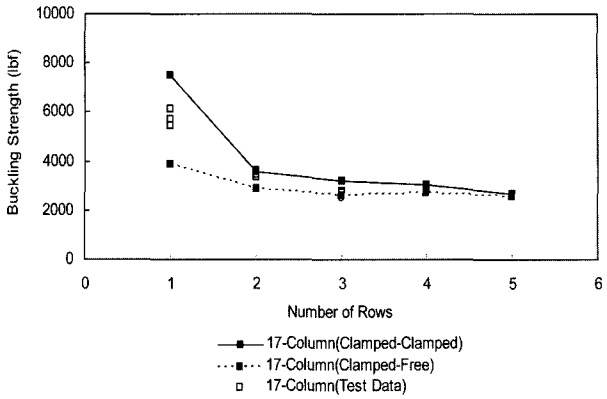

Fig. 12 Buckling Strengths as a function of the Number of Rows

consider the supporting effects by the slot and clamped conditions are applied for the lower part (Region A and D in Fig. 10) of the strap and welding location (Region C and F in Fig. 10) for the clamp-clamp boundary condition. The displacement constraints of lateral direction (Z-direction in strap models of Fig. 10) are released at Region D, E, F of strap models for the clamped-free boundary condition and the rotational constraints of lateral direction (Y direction in strap models of Fig. 10) are released at all Regions of strap models for the hinged-hinged boundary condition. The displacement coupling boundary conditions are applied for the all nodes at the boundary region with adjacent cell to consider the supporting effects by the slot of strap perpendicular to the load direction.

The static buckling strengths as a function of the number of straps (number of columns+1) for the cases of 1 and 2 rows with the clamped-clamped and clampeds-free condition, and for the case of 1 row with the hinged-hinged condition are shown in Fig. 11. Fig. 12 shows static buckling strengths as a function of the number of rows for the case of 17 columns for the clamped-clamped and clamped-free conditions. The analysis results are compared with the test data in Fig. 11 and Fig. 12. The buckling modes of 1, 2, 3, 4, and 5 strap models in vertical direction for the clamped-clamped and clamped-free conditions are shown in Fig. 13 and Fig. 14, respectively.

5. Discussions

5.1 The Effects of the Number of Rows and Columns

Fig. 5 shows the test results for the buckling strengths of grids as a function of the number of straps (number of columns+1) for the case of 1 and 2 rows. It was found that the buckling strengths of the small size grids that have 1 and 2 rows are linearly increased as the number of column increases. Based on the test data, the correlations between buckling strength and the number of straps for 1 row and 2 row cases are derived. It was evaluated that the buckling strength of small size grid can be predicted by using the buckling strength of unit grid that has the same number of rows with the small size grid. Fig. 11 shows the analysis and test results for the buckling strength of grids as a function of the number of columns (1~4 columns) for the case of 1 and 2 rows. The analysis results with clamped-clamped condition are a little higher than the test results and the analysis results with clamped-free condition are a little lower than the test results for the 1 row case. The test results for the 2 row case are a little lower than the analysis results with clamped-clamped condition and almost same

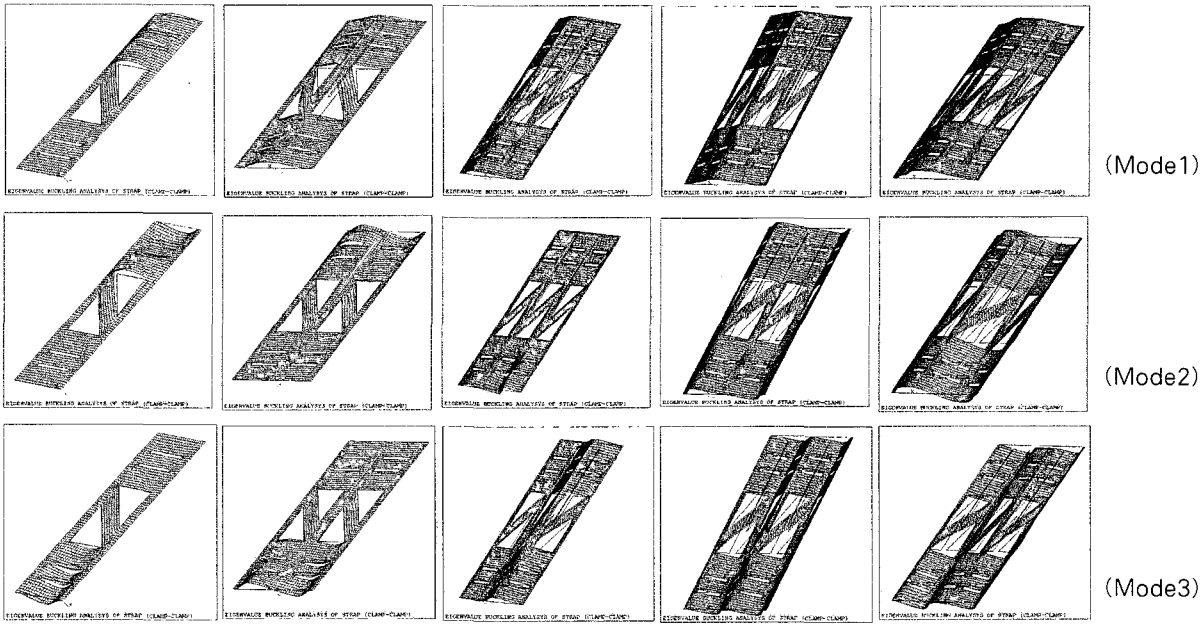

(a) 1 Strap Model (b) 2 Strap Mode (c) 3 Strap Mode (d) 4 Strap Mode (e) 5 Strap Mode

Fig. 13 Buckling Modes of Strap Models (Clamped Clamped Condition)

as the analysis results with clamped-free condition. There are large differences of buckling strength for the 1 row case and small differences of buckling strength for the 2 row case between clamped-clamped condition and clamped-free condition. It was evaluated that the large differences of buckling strength for the 1 row case are mainly due to the buckling mode differences between test results and analysis results. The buckling shapes of test results for 1 row grid in Fig. 4 are quite different from the buckling mode of analysis results for 1 strap model in Fig. 13(a). The buckling modes of 1 strap analysis results in Fig. 13(a) are strap deformation at upper part or lower part depend on the buckling mode, on the other hand the buckling shapes of test results in Fig. 4 are strap deformation at upper and lower part of the strap. The buckling analysis results with hinged hinged condition are compared with the test results in Fig. 11. It was evaluated that buckling strength of analysis results with hinged-hinged condition agree well with the buckling strength of test results. Moreover the buckling modes with hinged-hinged condition are same as the buckling shapes of the test results for 1 row grids in Fig. 4.

Fig. 6 shows the test results for the buckling strength of grids as a function of the number of rows for the case of 17 columns. It was found that the buckling strengths of small size grids and full size grids that have 17 columns are exponentially decreased as the number of row increases. Based on the test data, the correlations between buckling strength and the number of rows for 17 columns are derived. The effects of the number of rows on the buckling strength of spacer grids were more sensitive for the case of smaller number of rows and the effects are decreased as the number of row increases. There is only a little decrease of the buckling strength for the number of rows between 5 and 17 in Fig. 6. It was evaluated that the less sensitive effects of the number of rows on the buckling strength for the case of larger number of rows is mainly due to the buckling shapes. The buckling of the full size grid was occurred only at the 3 to 4 rows of grid as shown in Fig. 4 even though the full size grid has 17 rows. Fig. 12 shows the analysis and test results for the buckling strength

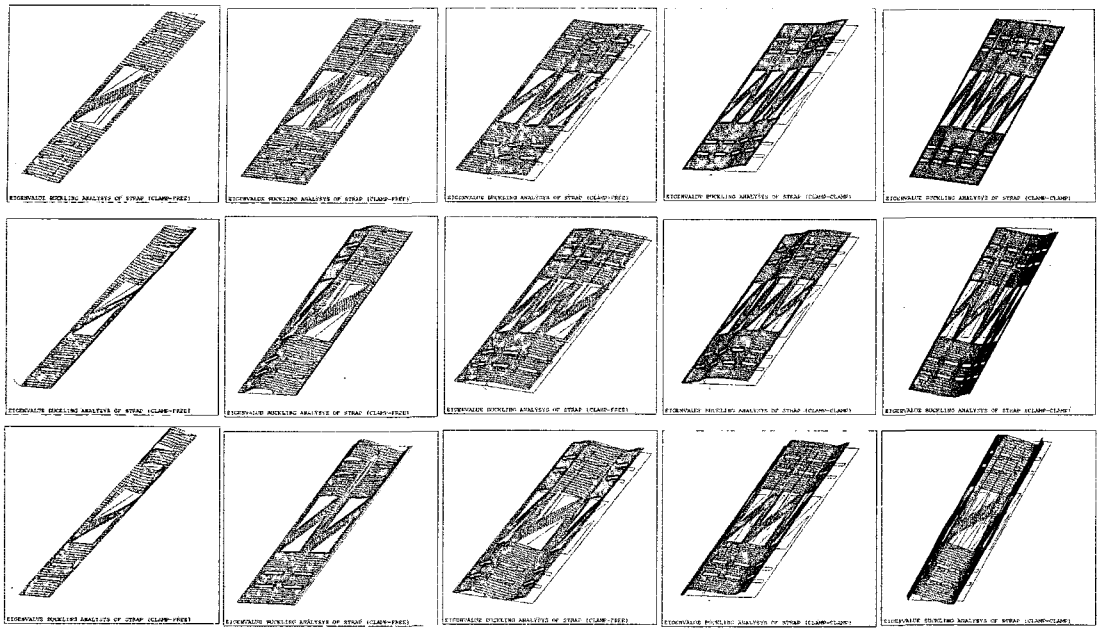

(a) 1 Strap Model (b) 2 Strap Mode (c) 3 Strap Mode (d) 4 Strap Mode (e) 5 Strap Mode

Fig. 14 Buckling Modes of Strap Models (Clamped-Free Condition)

of grids as a function of the number of rows for the 17 columns. There are large differences between test results and analysis results for the 1 row case and small differences between test results and analysis results for the 2 and 3 row cases. It was evaluated that the large differences of buckling strength for the 1 row case are mainly due to the horizontal sliding at the upper end of the vertical strap of 1×17 small size grids during buckling test. As a result of the sliding, the buckling strength was decreased compared to the expected buckling strength of 1×17 small size grids. The small differences of buckling strength for the 2 and 3 row cases are due to the same buckling mode between test results and analysis results. The buckling shapes of 2 and 3 row grids in Fig. 4 are same as the first buckling mode of 2 and 3 strap models in Fig. 13.

5.2 Buckling Mode

The buckling shapes of small size grids and full size grids from test results are shown in Fig. 4 and the buckling modes of strap from the analysis results are shown in Fig. 13 for clamped-clamped condition and in Fig. 14 for clamped-free condition. Each small size grid and full size grid has its own buckling shape depending on its configuration but the typical failure mode of small size grids and full size grids was a rotational failure at the welded position of grid strap intersects. The buckling shapes of test results for small size grids (2 row and 3 row grids) are same as the first buckling mode of the analysis results with clamped-clamped condition for 2 strap and 3 strap models as shown in Fig. 13, and the buckling shapes of test results for full size grids are same as the first buckling mode of the analysis results with clamped-free condition for 3 or 4 strap models as shown in Fig. 14. The buckling shapes of test results are strap deformation at upper and lower part of the strap for the 1 row grids, 1×1, 1×2, 1×3, 1×4 and 1×5, as shown in Fig. 4. However, the buckling modes of the analysis results with clamped-clamped condition for 1 strap model are strap deformation at upper part or lower parts depend on the buckling mode. The buckling modes with hinged-hinged condition are same as the

buckling shapes of the test results for 1 row grids in Fig. 4. The buckling location of the 2 row, 3 row, and full size grid is intersect of the strap and the number of buckled rows is depend on the size of the grids. The number of buckled row was 1 for 1 row grids, 2 for 2 and 3 row grids, 3 to 4 for full size grid. The buckling shapes of 1 row grids, 1×1, 1×2, 1×3, 1×4 and 1×5, 2 row grids, 2×1, 2×2, 2×3, and 2×9, and 3 row grid, 3×17 are same as the first buckling mode of the 1, 2, and 3 strap models for 1 row, 2 row, and 3 row grids, respectively, as shown in Fig. 4 and Fig. 13. The buckling shape of 1×17 specimens should be same as that of the 1 row grids, 1×1, 1×2, 1×3, 1×4 and 1×5 grids. However, there was some horizontal sliding at the upper end of the vertical strap of 1×17 small size grids during buckling test. As a result of the sliding, the buckling strength was decreased compared to the expected buckling strength of 1×17 small size grids and the buckling shape was different from the same kind of small size grids such as 1×1, 1×2, 1×3, 1×4 and 1×5. There were three different kind of buckling shapes for the full size grids as shown in Fig. 4. The buckling strengths are 1,452 lbf, 1,771 lbf, 1,965 lbf for buckling shape-1, buckling shape-2, and buckling shape-3 the of full size grids in Fig. 4, respectively. The buckling of the full size grid was occurred only at the 3 to 4 rows of grid as shown in Fig. 4 even though the full size grid has 17 rows. The buckling shape was 4 rows buckling at upper part and lower part of the full size grid for the buckling shape-1 in Fig. 4. The buckling shapes for buckling shape-2 and buckling shape-3 were 3 rows buckling at upper part and middle location of the full size grid, respectively. Most of the full size grids were buckled with buckling shape-1. And, the buckling strengths of full size grid were lowest values when the grid buckled with buckling shape-1. Based on the evaluation of buckling strength and buckling shape of 17×17 grids, the buckling shape of the grid should be considered for the evaluation of the buckling strength.

5.3 Prediction of Buckling Strength

Based on the test results, the correlations between buckling strength and the number of straps (number of columns+1) for 1 row and 2 row cases and the correlations between buckling strength and the number of rows for 17 columns were derived as shown in Fig. 5 and 6. The buckling strength of the small size grid that has several numbers of horizontal straps (or columns) can be predicted using the buckling strength of unit strap that has the same number of rows as shown in Fig. 5. And, the buckling strength of small size grid and full size grid that has several number of rows can be also predicted using the buckling strength of unit strap (or row) that has the same number of horizontal column as shown in Fig. 6. The buckling strength of the full size grid also can be predicted using the correlation between the buckling strength and the number of columns and the correlation between the buckling strength and the number of rows based on the analysis results as shown in Fig. 11 and 12. Even though there are some differences between analysis results and test results for the 1 row case, the buckling strength of the full size grid can be predicted based on the analysis results because the buckling of the full size grid will be occurred with the failure of more than 3 rows. As a result, the static buckling strength of the full size grids can be predicted by the test results of the small size grids and the analysis results for the number of columns and rows, and it can be used for the selection of a new grid model among various proposed ones considering buckling strength during the development of new grid design.

6. Conclusions

The buckling tests and finite element analyses were performed to evaluate the buckling characteristics of the spacer grids in a pressurized water reactor fuel assembly. The static buckling tests for small

size grids and full size grids were performed for the number of columns and rows. The static buckling analyses were also performed by a finite element method using ANSYS program and the results were compared with the buckling test results.

(a) The correlations between buckling strength and the number of straps for 1 row and 2 row cases and the number of rows for 17 columns are derived based on the average buckling strength from test results as shown in equations (2), (3), and (4).

(b) The buckling strengths of the small size grids that have 1 and 2 rows are linearly increased as the number of column increases and the buckling strengths of small size grids and full size grids that have 17 columns are exponentially decreased as the number of row increases.

(c) The buckling shapes of the small size grid that has the same number of row, 1 row grids, 2 row grids, and 3 row grids are same as the first buckling mode of the 1, 2, and 3 strap models for 1 row, 2 row, and 3 row grids, respectively.

(d) The buckling strength of the small size grid that has several numbers of horizontal straps (or columns) can be predicted using the buckling strength of unit strap that has the same number of rows. And, the buckling strength of small size grid and full size grid that has several numbers of rows can be also predicted using the buckling strength of unit strap (or row) that has the same number of horizontal column.

References

ANSYS Rev. 5.6 Swanson Analysis System Inc.

Han, T. H., Kim, J. S., Kim, J. H., Kang, Y. J. (2004) Elastic Shear Buckling of Curved Web Panels, *Journal of Computational Structural Engineering*, 17(2), pp.95~104.

Heo, S. P., Yang, W. H., Sung, K. D., Cho, M. R.(1999) A Study on the Buckling and Postbuckling Behaviors of Laminated Composite Plates and Stiffened Laminated Composite Panels by Finite Element Method, *Journal of Computational Structural Engineering*, 12(4), pp.599~606.

Hyun, M. H., Kim, U. N., Kim, B. J., Kim, W. S., Kim, D. H.(1997) A Study on the Fatigue and Buckling/Ultimate Strength of New Slot Hole Structure, *Proceedings of the Annual Autumn Meeting, SNAK*, pp 491~495.

KNFC(1994) Fuel Design Report for 17×17 Fuel Assembly, KNFC Proprietary.

Lee, J. S., Wang, X.(2002) Buckling of Ferromagnetic Plates in Thermal and Magnetic Fields, *Journal of Computational Structural Engineering*, 15(4), pp.727~739.

Lee, S. G., Kim, S. C., Song, Y. Y., Song, S. Y. (2002) Elastic Critical Loads of Rectangular Plates under Patch Loads, *Proceedings of Computational Structural Engineering Institute Fall Symposium*, pp.549~556.

Park, J. S, Ko, J. Y.(2004) Development of Buckling and Compressive Ultimate Strength Formulations for Rectangular Plate with Cutout, *Proceedings of Computational Structural Engineering Institute Fall Symposium*, pp.237~244.

USNRC(1981) Evaluation of Fuel Assembly Structural Response to Externally Applied Forces, USNRC Standard Review Plan Section 4.2 Appendix A.

Yoon, K. H., Kang, H. S., Kim, H. K., Song, K. N., Jung, Y. H.(2001) Nonlinear Dynamic Buckling Behavior of a Partial Spacer Grid Assembly, *Journal of the Korean Nuclear Society*, 33(1), pp.93~101.

Timoshenko, Gere(1982) Theory of Elastic Stability, *McGraw Hill*.